A COLLISIONLESS E × B INSTABILITY WITH LARGE ION ORBITS

Francis F. Chen
Electrical Engineering Department and
Institute of Plasma and Fusion Research
University of California, Los Angeles
Los Angeles, CA 90024-1594, U.S.A.

Introduction

A flute instability of a partially ionized, magnetized plasma with a transverse electric field was shown by Simon /1/ and Hoh /2/ to be responsible for the violent instability of reflex discharges which allows electron current to cross the magnetic field. The main cause of this instability is the difference between the electron and ion $\mathbf{E} \times \mathbf{B}$ drifts due to ion-neutral drag. This effect is not present in collisionless plasmas, but the instability is still found if the ion drift is slowed by the finite Larmor radius effect /3//4/. In a recent experiment by Sakawa /5/, clear evidence of this collisionless instability was found in a plasma which was much smaller than the ions' Larmor radii. The observed frequency was much higher than the ion cyclotron, diamagnetic drift, and $\mathbf{E} \times \mathbf{B}$ frequencies, thus eliminating both the $\mathbf{E} \times \mathbf{B}$ and the drift instabilities. The ions trapped in the potential well of the E-field had nearly straight-line orbits, with only a small curvature due to the Lorentz force. The ion fluid then has an $\mathbf{E} \times \mathbf{B}$ drift much smaller than that of the electrons, even though there are no collisions.

It is easy to show that such a fluid suffers from a strong flute (not drift) instability with a phase velocity close to that of the slow ion drift, as observed. The equilibrium, however, has to be treated kinetically, since the system is much smaller than the ion orbits; and it is the equilibrium which is difficult to treat. An expansion in a small Larmor radius parameter would not be suitable; rather, the curvature of the ion orbits is the small quantity. By choosing a particular functional form for the electric field profiles, we have found a simple way to model the equilibrium in both plane and cylindrical geometries. The cylindrical case is applicable to beam-plasma experiments /5/, while the plane case can be used to devise experiments to clarify the edge physics in tokamak H-mode boundary layers which are thinner than the ion Larmor radius.

Equilibrium: plane geometry

Consider a plasma confined between infinite planes at $x = \pm L$, embedded in a uniform magnetic field $\mathbf{B} = B_0 \hat{z}$. A jet-like $\mathbf{E} \times \mathbf{B}$ velocity distribution in the y direction in the slab can be modeled by the following analytic functions:

$$\phi = \phi_0 \tanh \xi \tag{1}$$

$$\mathbf{E} = -(N/L)\,\phi' \hat{x} = -(N/L)\,\phi_0 \operatorname{sech}^2 \xi \, \hat{x} \tag{2}$$

$$\rho = (N/L)\,\varepsilon_0 E_x' = 2\varepsilon_0 (N/L)^2 \,\phi_0 \operatorname{sech}^2 \xi \tanh \xi \quad , \tag{3}$$

where

$$\xi \equiv Nx/L \quad , \tag{4}$$

ϕ is the potential, ρ is the charge density, and N is a parameter for adjusting the sharpness of the profile. These profiles are shown in Fig. 1 for $N = 2$. We take $\phi_0 > 0$, so that $E_x < 0$,

and ions are driven to the left. The magnetic field is so weak that the ions bounce between their birthplace and the left wall in nearly straight lines, but there is a small curvature to the orbits, giving the ions a drift in the y direction. For a tokamak edge layer, the left boundary would be the main plasma, and the right boundary would be the first wall. For a cylindrical beam-plasma experiment, the left boundary would simulate the axis, and the right boundary would be the wall.

We next construct a density profile that is consistent with this potential profile. Let $v(\xi, \xi_0)$ be the velocity of an ion, located at ξ, which was born (at rest) at ξ_0. Its kinetic energy $\frac{1}{2}Mv^2(\xi, \xi_0)$ is gained from the potential drop between ξ_0 and ξ. Thus,

$$v^2(\xi, \xi_0) = (2e\phi_0 / M)(\tanh\xi_0 - \tanh\xi) \quad . \tag{5}$$

The y component of the ion equation of motion reads

$$dv_y / dt = -(e/M)\, v_x B = -\Omega_c v_x \quad , \tag{6}$$

where Ω_c is the ion cyclotron frequency. The Lorentz force accelerates the ions in the y direction at the rate

$$\frac{dv_y}{dt} = \frac{dv_y}{dx}\frac{dx}{dt} = \frac{dv_y}{dx} v_x \qquad \therefore \frac{dv_y}{dx} = -\Omega_c \quad . \tag{7}$$

The velocity v_y of an ion at ξ which was born at ξ_0 is thus

$$v_y(\xi, \xi_0) = -\Omega_c(x - x_0) = (L/N)\,\Omega_c(\xi_0 - \xi) \quad . \tag{8}$$

Note that this depends only on position; it is independent of the strength of the E-field. Combining Eqs. (7) and (10), we find for the x velocity component,

$$v_x^2(\xi, \xi_0) = v^2 - v_y^2 = (2e\phi / M)(\tanh\xi_0 - \tanh\xi) - (L\,\Omega_c / N)^2(\xi_0 - \xi)^2 \quad . \tag{9}$$

Let the ions be created at a rate $S(x_0)$ m^{-3} sec^{-1}. Since the flux nv_x is conserved, the density at x due to a source $S(x_0)\,dx_0$ is proportional to $1/|v_x(x, x_0)|$. The constant of proportionality is 0, 1, or 2, depending on whether the ion is turned around before reaching x, is absorbed at the left boundary, or is reflected at $-L$ or turned around at a radius between $-L$ and x. For simplicity we assume a reflecting boundary. Integrating over all source positions upstream of x and changing to the variable ξ, we obtain

$$n(\xi) = \frac{2L}{N}\int_{\xi}^{\xi_{\max}} \frac{S(\xi_0)d\xi_0}{|v_x(\xi, \xi_0)|} \quad . \tag{10}$$

Here, $\xi_{\max}$ is the smaller of N and that value of ξ_0 beyond which v_x^2, given by Eq. (9), becomes negative, indicating that the ion turns around before ξ. One needs only to end the integration when v_x becomes imaginary. The integrand is singular at two points: $\xi = \xi_0$, and $v^2 = v_y^2$, but these are obviously integrable singularities because the density physically has to be finite if the source S is finite. The experimental density profile can be matched by choosing a suitable function $S(\xi_0)$. Fig. 2 shows sample n_1 profiles which are consistent with Eq. (1).

To obtain the ion fluid drift v_{0y} at any position x, we need only to sum over all source positions the values of $v_y(\xi, \xi_0)$, given by Eq. (8), weighted by the source strength $S(\xi_0)$ and the residence time $1/|v_x|$, and normalize:

$$v_0(\xi) = \frac{2}{n(\xi)}\int_{\xi}^{\xi_{\max}} v_y(\xi, \xi_0)\,\frac{S(\xi_0)\,d\xi_0}{|v_x(\xi, \xi_0)|} \quad . \tag{11}$$

The corresponding profiles of v_0 are also shown in Fig. 2.

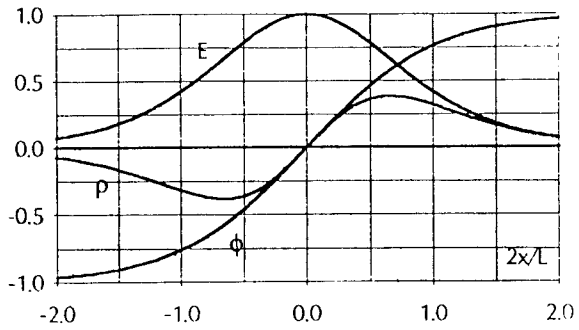

Fig. 1

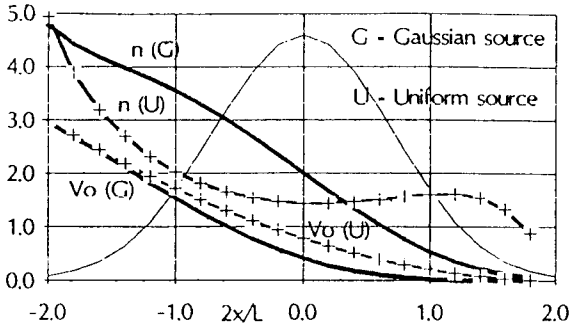

Fig. 2

Equilibrium: cylindrical geometry

In the experiment in question /5/, a beam of electrons injected along the axis depresses the potential there and gives rise to a nonuniform radial electric field. The corresponding sheared $\mathbf{E} \times \mathbf{B}$ drift is in the θ direction and falls to zero at $r = 0$ and $r = a$. This situation can be modeled by a consistent set of Bessel functions:

$$\phi = -\phi_0 [J_0(Tr) - J_0(w_1)] \tag{12}$$

$$E_r = -\frac{\partial \phi}{\partial r} = \phi_0 \frac{\partial}{\partial r} J_0(Tr) = -\phi_0 T J_1(Tr) \tag{13}$$

$$\rho = \varepsilon_0 \frac{\partial}{\partial r}(r E_r) = -\varepsilon_0 \phi_0 T^2 J_0(Tr) \quad , \tag{14}$$

where w_1 is a zero of J_1 ; for instance, the first zero is $w_1 = 3.83$. That Eq. (16) is true can be verified by substituting for E_r from Eq. (15), taking the r-derivative of ρ in both parts of the equation, and recognizing the differential equation that defines J_1. Setting $T = w_1/a$ ensures that both ϕ and E_r vanish at $r = a$. These profiles are shown in Fig. 3.

The kinetic energy $\frac{1}{2}Mv^2(r, r_0)$ of an ion at r which was born at rest r_0 has been gained from the potential drop between r_0 and r. Defining $z = Tr$, we can therefore write

$$v^2(z, z_0) = \frac{2e\phi_0}{M} [J_0(z) - J_0(z_0)] \quad . \tag{15}$$

The Lorentz force curves the ion orbits, which would otherwise be straight lines through the axis, as the ions bounce in the dc potential well. The θ component of velocity can be found from the conservation of canonical angular momentum:

$$P_\theta = Mrv_\theta + \tfrac{1}{2} e B_0 r^2 = \tfrac{1}{2} e B_0 r_0^2 \quad , \tag{16}$$

where $\frac{1}{2}B_0 r$ is the vector potential A_θ in a uniform field, and we have taken (for the time being) v_θ to be zero at $r = r_0$. Solving for v_θ, we have

$$v_\theta(z, z_0) = \frac{\Omega_c}{2T} \frac{z_0^2 - z^2}{z} \quad . \tag{17}$$

Eqs. (15) and (17) give

$$v_r^2(z, z_0) = v^2 - v_\theta^2 = \frac{2e\phi_0}{M} [J_0(z) - J_0(z_0)] - \left(\frac{\Omega_c}{2T}\right)^2 \left(\frac{z_0^2 - z^2}{z}\right)^2 \quad . \tag{18}$$

To calculate the density, we again integrate over a source distribution $S(z_0)$, weighted by the residence time $1/|v_r|$ and a geometrical compression factor z_0/z due to the cylindrical geometry:

$$n(z) = 2\int_z^{z_{max}} \frac{z_0}{z} \frac{S(z_0)\,dz_0}{|v_r(z, z_0)|} \quad . \tag{19}$$

Here, z_{max} is the smaller of w_1 and the value of z_0 at which v_r^2, given by Eq. (18), is zero; beyond that, the ions do not reach z. Since all ions are "reflected", they contribute twice to the density at any radius. The factor 2 included for this is not important, since $S(z_0)$ is to be adjusted to fit the experiment anyway. The fluid drift v_0 in the θ direction is given by the weighted average of v_θ, as given by Eq. (17):

$$v_0(z) = \frac{2}{n(z)} \int_z^{z_{max}} v_\theta(z, z_0) \frac{z_0}{z} \frac{S(z_0)\,dz_0}{|v_r(z, z_0)|} \quad . \tag{20}$$

Examples of n and v_0 profiles are given in Fig. 4.

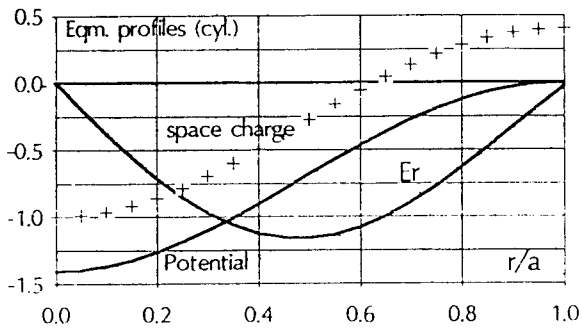

Fig. 3

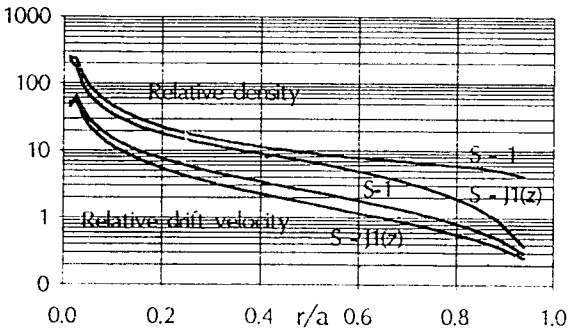

Fig. 4

Although the ions are born with very little energy, a small amount of angular momentum at large radii could greatly affect the ions' turnaround radius, and thus the density at small radii. To examine this effect, we can add a thermal velocity $v_\theta(r_0) = \pm v_t$. A term $mrv_\theta(r_0)$ is then added to Eq. (16), resulting in a term $v_\theta(r_0)$ added to Eq. (17), with corresponding changes in subsequent equations. The results, which we cannot show here, indicate that $v_\theta(r_0)$, has more effect when it is in the same direction as the Lorentz force, but that the effect is small unless $\frac{1}{2}Mv_\theta^2$ is comparable to $e\phi_0$.

The instability

Since the instability is basically a fluid effect, we use the fluid equations. We confine ourselves here to plane perturbations of the form $\exp i(ky - \omega t)$. For the ions, the linearized equations are:

$$M\left(\frac{\partial \mathbf{v}}{\partial t} + \mathbf{v}_0 \cdot \nabla \mathbf{v} + \mathbf{v} \cdot \nabla \mathbf{v}_0\right) = e(\mathbf{E} + \mathbf{v} \times \mathbf{B}_0) \tag{21}$$

$$\frac{\partial n}{\partial t} + n_0 \nabla \cdot \mathbf{v} + \mathbf{v} \cdot \nabla n_0 + n \nabla \cdot \mathbf{v}_0 + \mathbf{v}_0 \cdot \nabla n = 0 \quad . \tag{22}$$

Here, $v_0(x)$ is the averaged velocity computed above. From the electron equations, we obtain the modified Boltzmann relation /6/ appropriate for $k_{||} = 0$ and finite ∇n_0 and E_0:

$$\frac{n}{n_0} = \frac{e\phi}{KT_e} \frac{\omega_*(x)}{\omega - \omega_E(x)} \quad . \tag{23}$$

Here, ω_* is the electron diamagnetic drift frequency $-k(KT_e/eB_0)\,n_0'/n_0$, and ω_E is the $\mathbf{E} \times \mathbf{B}$ drift frequency $-kE_0/B_0$. Solving Eq. (21) for the first-order ion fluid velocity $\mathbf{v}$,

substituting into Eq. (22), and eliminating n with Eq. (23), we obtain a second-order differential equation for $\phi(x)$. We keep all x-derivatives ($'$) in both zero- and first-order quantities. The result can be written in the form

$$\phi'' + f(x)\phi' + g(x)\phi \;=\; 0 \quad . \tag{24}$$

Defining $\varpi(x) = \omega - kv_0(x)$ and

$$\delta(x) \;=\; n_0'(x)\,/\,n_0(x)\,, \qquad \gamma(x) \;=\; \frac{2\varpi k v_0' + \Omega_c v_0''}{\varpi^2 - \Omega_c(\Omega_c + v_0')} \quad , \tag{25}$$

we can write the coefficients as

$$f(x) \;=\; \delta(x) + \gamma(x) \tag{26}$$

$$-g(x) \;=\; k^2\left[1 + \frac{\Omega_c}{\varpi}\,\frac{\delta+\gamma}{k} + \frac{\delta}{k}\,\frac{\varpi^2 - \Omega_c(\Omega_c + v_0')}{\Omega_c(\omega - \omega_E)}\right] \quad , \tag{27}$$

where all the quantities are x-dependent except k, Ω_c, and ω. Eq. (24) is to be integrated between $-L$ and L using the self-consistent profiles of n_0, E_0, and v_0 computed above to obtain the eigenvalues of ω. By eliminating the velocity shear terms, one can study the Kelvin-Helmholtz effect on this instability.

The basic instability can be uncovered by making the local approximation $g(x) = 0$. This yields a cubic equation for ϖ:

$$\varpi^3 + (k\,/\,\delta)\,\Omega_c\,(\varpi^2 - \omega_d\varpi) - \Omega_c^2\,\omega_d \;=\; 0 \quad , \tag{28}$$

where

$$\omega_d \;=\; \omega_E - kv_0 \tag{29}$$

is the difference between the electron and ion $\mathbf{E}\times\mathbf{B}$ drifts. The unstable root can be seen by taking the limit $\omega_E \gg \Omega_c$ and small v_0, so that $\varpi \approx \omega_d \approx \omega_E$. The last term in Eq. (28) can then be neglected; and, for $n_0'\,/\,n_0 < 0$, the resulting quadratic equation yields

$$\omega \;=\; kv_0 + k\Omega_c/2|\,\delta\,| + i(k\,\Omega_c\,\omega_d\,/\,|\,\delta\,|)^{1/2} \quad . \tag{30}$$

The frequency is of order kv_0, and the growth rate depends on the difference between electron and ion drifts in the equilibrium.

/1/ A. Simon, *Phys. Fluids* 6, 382 (1963).

/2/ F.C. Hoh, *Phys. Fluids* 6, 1184 (1963).

/3/ M.N. Rosenbluth, N.A. Krall, and N. Rostoker, *Nucl. Fusion Suppl.*, Part 1, 143 (1962).

/4/ F.F. Chen, *Phys. Fluids* 9, 965 (1966).

/5/ Y. Sakawa, *Thesis*, UCLA (1992).

/6/ R.W. Motley, *Q Machines*, p. 49, Academic Press, New York (1975).